Toroidal drift modes driven by ion pressure gradients

Wendell Horton, Duk-In Choi, and W. M. Tang

Citation: The Physics of Fluids **24**, 1077 (1981); doi: 10.1063/1.863486
View online: https://doi.org/10.1063/1.863486
View Table of Contents: https://aip.scitation.org/toc/pfl/24/6
Published by the American Institute of Physics

ARTICLES YOU MAY BE INTERESTED IN

Electron temperature gradient driven turbulence
Physics of Plasmas **7**, 1904 (2000); https://doi.org/10.1063/1.874014

Ion temperature-gradient-driven modes and anomalous ion transport in tokamaks
Physics of Fluids B: Plasma Physics **1**, 1018 (1989); https://doi.org/10.1063/1.859023

Instabilities due to Temperature Gradients in Complex Magnetic Field Configurations
The Physics of Fluids **10**, 582 (1967); https://doi.org/10.1063/1.1762151

Comparisons and physics basis of tokamak transport models and turbulence simulations
Physics of Plasmas **7**, 969 (2000); https://doi.org/10.1063/1.873896

Nonlinear gyrokinetic equations for low-frequency electromagnetic waves in general plasma equilibria
The Physics of Fluids **25**, 502 (1982); https://doi.org/10.1063/1.863762

Influence of sheared poloidal rotation on edge turbulence
Physics of Fluids B: Plasma Physics **2**, 1 (1990); https://doi.org/10.1063/1.859529

Toroidal drift modes driven by ion pressure gradients

Wendell Horton, Jr.
Institute for Fusion Studies, The University of Texas at Austin, Austin, Texas 78712

Duk-In Choi
Korea Advanced Institute of Science, Chongyangni, Seoul, Korea

W. M. Tang
Plasma Physics Laboratory, Princeton University, Princeton, New Jersey 08544
(Received 14 March 1980; accepted 27 February 1981)

Ion pressure gradient-driven drift modes are analyzed for their parametric dependence on the shear, the toroidal aspect ratio, and the pressure gradient using the ballooning toroidal mode theory. An approximate formula for the anomalous ion thermal conductivity is derived for the turbulent regime.

I. INTRODUCTION

In view of the high ion temperatures now being produced by powerful auxiliary heating in tokamaks, it is interesting to re-examine the ion pressure gradient driven drift modes along with their associated anomalous thermal transport. In this article we analyze the mode structure of these pressure gradient driven modes using the recently developed methods for studying toroidal drift modes.[1-5] The parametric variation with toroidal curvature, magnetic shear and the pressure gradient of the unstable mode characteristics, such as their angular width, average radial and parallel wavenumbers, is investigated in an effort to elucidate features that could be useful for their identification in fluctuation measurements.

Let us briefly contrast the pressure gradient instability with the results known from earlier studies of the drift wave[1,2] and the trapped electron mode.[6] With a low ion pressure gradient, the toroidal drift wave is trapped on the outside of the torus for the shear parameter $\xi = rq'/q < \frac{1}{2}$, and the solution of the eigenvalue problem yields a destabilizing frequency shift. For $\xi > \frac{1}{2}$ the modes shift their position of maximum amplitude[1,2] and become weakly localized for $(k\rho)^2\xi \lesssim \epsilon_n$. In this transitional regime there is a weak shear damping determined by tunneling of the wavefunction through an evanescent region. For still larger shear-to-toroidicity ratios the well-known slab model shear damping reappears. Now as the ion pressure gradient becomes finite another branch of oscillation is added to the system.[7] When the ion pressure gradient becomes strong, $T_i \gtrsim T_e$ and $\nabla \ln T_i > \nabla \ln n_i$, the two modes of oscillation merge into complex conjugate pairs to produce a strong fluid-like instability.[8]

The drift mode analyzed here is driven by the geometric mean of the ion pressure gradient and the unfavorable magnetic curvature. In the shearless multipole configuration the effect of ballooning and the downward shift in the drift wave oscillation frequency are known[9] to occur from the field line variation of the ion curvature drifts and are aspects of the present stability analysis. In its ballooning and maximum growth rate the pressure gradient driven drift mode is similar to its long wavelength magnetohydrodynamic counterpart.[10] The cross-field wavelength for the drift mode scales with the ion gyroradius in contrast to the macroscopic scale of the magnetohydrodynamic mode. In both regimes the growth rate is required to exceed the thermal ion transit frequency for applicability of the hydrodynamic approximation.

In Sec. II we analyze the toroidal normal mode equation. In Sec. III we investigate the parametric variation of the instability and compare the numerical integration with the appropriate formulas. In Sec. IV we construct a mode coupling theory for the nonlinear regime of the instability. We obtain a model for the azimuthal mode number spectrum in the turbulent state. In Sec. V we evaluate the anomalous ion thermal flux implied by the fluctuation spectrum.

II. NORMAL MODE PROBLEM

In a previous study[1] of the ballooning drift modes we reduced the normal mode problem to the Sturm–Liouville equation by considering the first order frequency shift $\Delta\omega$ produced by the finite toroidal geometry. In that analysis we first introduce the frequency ω_k defined by the shearless slab approximation to the system and then derive the differential equation for the finite geometry mode with the Sturm–Liouville eigenvalue $\lambda_{SL} = \Delta\omega\omega_*/\omega_k^2$ determined by the balance of the toroidal curvature, the shear, and the two dimensional wave propagation. Figure 5 of Ref. 1 shows the variation of $\lambda_{SL} = \Delta\omega\omega_*/\omega_k^2$ for the electron drift wave with fixed ϵ_n and k_0 as a function of shear. The Sturm–Liouville approximation is justified for parameters which lead to small $\Delta\omega/\omega_k$. As the frequency shift $\Delta\omega$ becomes comparable to the slab wave frequency ω_k, however, the approximation fails.

In the investigation of the ion pressure gradient mode it becomes apparent that the toroidal drift mode frequency $\omega_k(\nabla p_i)$ is substantially reduced from the slab model, ω_k, and consequently the small $\Delta\omega/\omega_k$ approximation is inadequate. In fact, for $\eta_i = d\ln T_i/d\ln n_i \gtrsim 1$, the fastest growing perpendicular wavenumber in the slab occurs for $k_\perp^2\rho^2 \simeq (1-2\epsilon_n)/(1+\eta_i)$, where the drift mode frequency depends on the toroidal curvature as $\epsilon_n^{1/2}$. Consequently the full nonlinear ω dependence of the toroidal ion drifts and the ion acoustic terms must be retained. In this regime the normal mode equation for the ballooning representation function $f(y)$ defined in Ref. 1 is found to be

 0031-9171/81/061077-09$00.90 © 1981 American Institute of Physics

$$\frac{d^2f(y)}{dy^2}+\frac{q^2\omega^2}{\epsilon_n^2}\left(\frac{\omega-k}{\omega+k(1+\eta_i)}+\frac{2\epsilon_n k}{\omega}K(y,y_0)\right.$$
$$\left.+k^2[1+\xi^2(y-y_0)^2]\right)f(y)=0\,, \tag{1}$$

where $K(y,y_0)=\cos y+\xi(y-y_0)\sin y$. We seek solutions of Eq. (1) which for large y^2 approach the asymptotic solution

$$f_+(y^2)=A_+\exp[(iqk\xi\omega/2\epsilon_n)y^2]\,,$$

which is exponentially convergent for ω in the growing part of the complex plane. In contrast to the Sturm–Liouville problem that governs the frequency shift $\Delta\omega$, the different axial modes of the normal mode problem given by Eq. (1) are not orthogonal. The sequence of modes $[\omega_n, f_n(y)]$ is linearly independent and forms a complete set with respect to nonsingular initial perturbations. In Eq. (1) the dimensionless variables[1,5] are given by $k=k_\perp\rho$, $\omega=\omega r_n/c_s$, $\epsilon_n=r_n/R$, $q=rB/RB_\theta$, and $\xi=rq'/q$ and are defined in more detail in Refs. 1 and 5.

We now proceed to obtain approximate solutions of Eq. (1) in the strong mode coupling approximation and compare the results with numerical integrations. We consider modes that are localized to the outside of the torus where $K(y,y_0=0)\simeq 1+(\xi-\frac{1}{2})y^2$. In this case the solutions of Eq. (1) are

$$f_m(y)=H_m(\sigma_m y)\exp(-\tfrac{1}{2}\sigma_m y^2)\,,$$

where $\sigma_m=\sigma(\omega_m)$ with

$$\sigma(\omega)=\frac{q\omega}{\epsilon_n}\left[\frac{2\epsilon_n k}{\omega}\left(\frac{1}{2}-\xi\right)-k^2\xi^2\right]^{1/2}, \tag{2}$$

and the eigenfrequency for $f_m(y)$ is given by

$$D(\omega)=\frac{\omega-k}{\omega+k(1+\eta)}+\frac{2\epsilon_n k}{\omega}+k^2$$
$$=\frac{\epsilon_n(2m+1)}{q\omega}\left[\frac{2\epsilon_n k}{\omega}\left(\frac{1}{2}-\xi\right)-k^2\xi^2\right]^{1/2}. \tag{3}$$

Although it is straightforward to solve the dispersion relation (3) numerically, we find it satisfactory for the present analysis to consider the right-hand side of Eq. (3) as a perturbation. We then obtain

$$\omega(k,m)=\omega_\pm^0(k)+\Delta\omega_\pm(k,m)\,, \tag{4}$$

where

$$\omega_\pm^0(k)=\frac{k}{2(1+k^2)}\left(1-2\epsilon_n-k^2(1+\eta)\pm\{[1-2\epsilon_n-k^2(1+\eta)]^2\right.$$
$$\left.-8\epsilon_n(1+\eta)(1+k^2)\}^{1/2}\right)\,, \tag{5}$$

and the frequency shift is

$$\Delta\omega_\pm(k,m)=\frac{\epsilon_n(1+2m)}{q\omega(\partial D/\partial\omega)}\left[\frac{2\epsilon_n k}{\omega}\left(\frac{1}{2}-\xi\right)-k^2\xi^2\right]^{1/2}\Bigg|_{\omega=\omega_\pm^0(k)}. \tag{6}$$

The lowest order eigenfrequency (5) is independent of shear and agrees with Eq. (28) of Ref. 8 when trapped electron effects are neglected. From Eq. (5) we see that the lowest order frequency becomes complex for $8\epsilon_n(1+\eta_i)(1+k^2)>[1-2\epsilon_n-k^2(1+\eta)]^2$ which is satisfied for modes with $k^2\lesssim(1-2\epsilon_n)/(1+\eta_i)$. The contribution of the complex frequency shift $\Delta\omega(k,m)$ to $\gamma=\mathrm{Im}\,\omega$ is less important than the lowest order growth rate obtained from Eq. (5). For the faster growing modes, Eq. (5) gives the growth rate

$$\gamma_k\cong\frac{\sqrt{2}\,k\epsilon_n^{1/2}(1+\eta)^{1/2}}{(1+k^2)^{1/2}} \tag{7}$$

proportional to the geometric mean of the unfavorable toroidal curvature and the ion pressure gradient.

Now it is instructive to consider the slab limit of the dispersion relation (3). The slab limit $\epsilon_n\to 0$ and $q\to 0$ such that ϵ_n/q is finite. Taking $(-k^2\xi^2)^{1/2}\to -ik\xi$ the quadratic dispersion relation for the sheared plasma slab obtained by Coppi *et al.*[7] is obtained. The two roots are

$$\omega_\pm^S(k)=[k/2(1+k^2)](1-k^2(1+\eta)-iS$$
$$\pm\{[1-k^2(1+\eta)-iS]^2-4iS(1+\eta)(1+k^2)\}^{1/2})\,,$$

where $S=\xi\epsilon_n/q=r_n/L_s$. The fastest growing modes occur in approximately the same wavenumber domain as in the toroidal problem, but the frequency is now comparable to the growth rate as given by

$$\omega_k+i\gamma_k\simeq\frac{1+i}{\sqrt{2}}\,\frac{kS^{1/2}(1+\eta)^{1/2}}{(1+k^2)^{1/2}}\,. \tag{8}$$

The relationship between the toroidal mode given in Eq. (7) and the slab mode in Eq. (8) is shown in Fig. 1. From the analysis it is evident that the growth rate varies continuously from (7) to (8) as S exceeds $2\epsilon_n$ or, equivalently, as $\xi>2q$. Typical tokamak plasma parameters fall well into the toroidal domain in Fig. 1.

In the toroidal regime the real frequency is smaller than the growth rate and is calculated by including the contribution from $\Delta\omega_\pm(k,m)$. The growth rate formula (7) shows the relationship between these kinetic modes with $k_\perp\rho$ of order unity and the pressure gradient driven ballooning magnetohydrodynamic modes[10] which have $k_\perp\rho\sim\rho/r_n$. In the magnetohydrodynamic ballooning mode there is no shielding of the dynamics by adiabatic electrons, and the ion and electron pressure gradients add together due to both species having the same dynamics. We

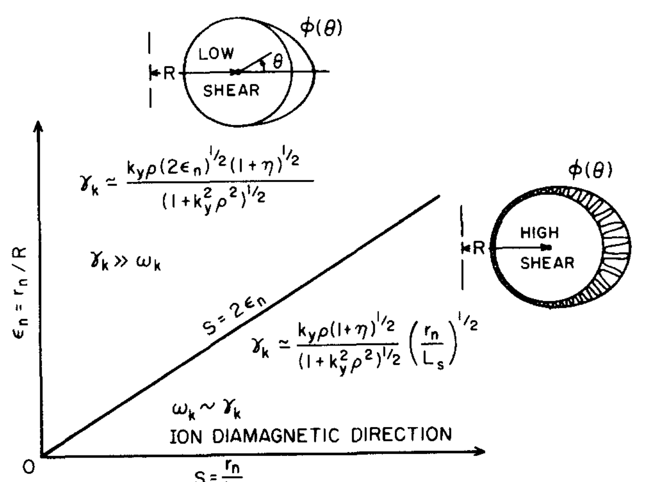

FIG. 1. A diagram showing the transition from the toroidal ballooning mode to the high-shear slab mode of Ref. 7. The changing character of the parallel wave function $\phi(\theta)$ is also indicated.

recover the magnetohydrodynamic growth rate when these changes are made *ad hoc* in Eq. (7). In Fig. 2 we show the mode frequency obtained from Eq. (5) compared with the value obtained from numerical integration of the eigenvalue problem (1) as a function of the azimuthal wavenumber. We see, for example, that for the growing mode $\omega^0(k=0.6) = -0.0485 + i0.5122$ given by (5) that $\Delta\omega(k, m=0)$ is of the order of a few percent of $\gamma^0(k)$. The numerical integration yields an $\omega(k, m=0)$ which agrees with $\omega^0 + \Delta\omega$ to within a few parts in a hundred in most cases. The influence of the $\Delta\omega$ term (8) is greatest at the branch point shown near $k\rho \simeq 1.4$ in Fig. 2.

III. PARAMETRIC DEPENDENCE OF THE NORMAL MODE GROWTH RATE AND WAVEFUNCTIONS

In the previous study of the low ion temperature equation the modes are shown to be strongly localized to the outside of the torus only for $\xi < \frac{1}{2}$. A typical mode at larger shear, $\xi = 1$, is shown in Fig. 4 of Ref. 1 to have a small oscillatory wavefunction extending to large y^2. The low ion temperature equation is recovered from Eq. (1) in the limit $\eta_i \to -1$. In this limit the (+) root reduces to the drift wave with $\omega_+ \simeq k(1-2\epsilon_n)/(1+k^2)$ and the (−) root to a toroidal mode with $\omega_- \simeq 2k\epsilon_n(1+\eta)/(1+k^2)(1-2\epsilon_n)$.

For $\eta_i \approx 1$, the eigenvalues and wavefunctions determined by Eq. (1) are qualitatively different from the low ion temperature modes. The modes with finite ion pressure gradient are more strongly localized to the outside of the torus even at large shear. As a result the wave energy is trapped and the modes now grow even in the absence of electron dissipation ($\delta_k^e = 0$). The growth rate is found to be described adequately by Eq. (7) over the range of parameters $(k, \epsilon_n, \xi, \eta_i)$ of most physical interest.

When the ion pressure gradient is sufficient to drive localized modes in a torus with $\mathrm{Re}(\omega^2) = \omega_k^2 - \gamma_k^2 < 0$, the asymptotic behavior of the wavefunctions no longer gives rise to an outward propagation of wave energy. Thus, the shear damping mechanism is defeated by the toroidal localization of the ion pressure gradient and bad curvature driven modes.

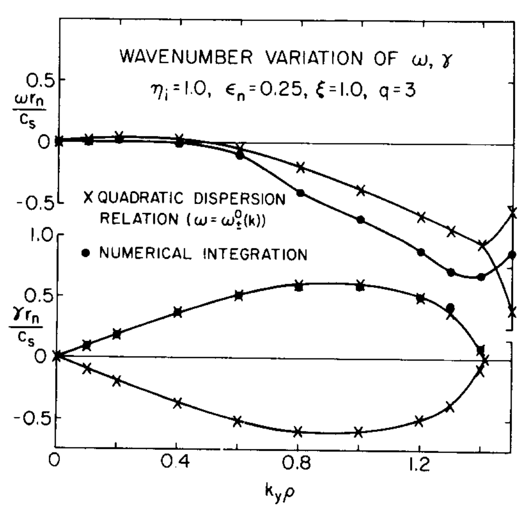

FIG. 2. The variation of ω_k, γ_k with azimuthal mode number obtained from the dispersion relation (3) and the normal mode equation (1) is shown.

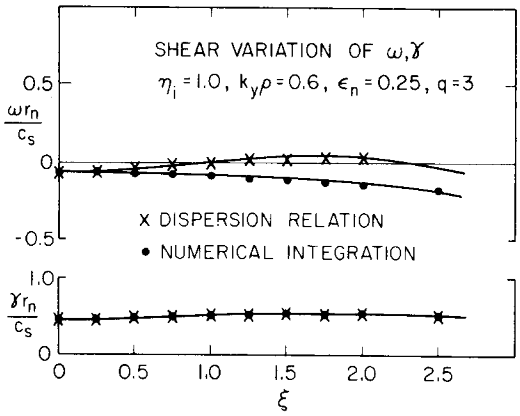

FIG. 3. Shows the variation of ω_k, γ_k with shear as obtained from the dispersion relation and the numerical integration. The variation is weak for $\xi < 2q$.

We confirm that Eq. (7) adequately represents the growth rate of the η_i modes by considering parameter variations from the reference case with $\epsilon_n = 1/4$, $\xi = 1$, $\eta_i = 1$, $q = 3$, and $k = 0.6$. For the reference case, formula (7) gives $\gamma(k=0.6) = 0.514$. Numerical solutions with variations for $\epsilon_n = 1/8$ to $1/2$; $\xi = 0$ to 2; $\eta_i = 0$ to 2.0; $q = 1.4$; and $k = 0.2$ to 1.4 show good agreement with formula (7). The complex frequency shift given by Eq. (6) is important in calculating the mode frequency but not the growth rate.

Figure 3 verifies that the growth rate obtained from the numerical integration of Eq. (1) is nearly independent of the shear in the toroidal domain ($\xi < 2q$) of Fig. 1. The growth rate given in Fig. 3 agrees well with that obtained from the simple formula (7), while the lowest order frequency formula $\omega^0(k)$ is sufficient only for $\xi < 1$. For $\xi > 1$ the normal mode frequency increases weakly with shear while rotating in the ion diamagnetic direction. For the reference parameters the rotational velocity is approximately one-half the ion diamagnetic drift speed.

Figure 4 verifies that the growth rate increases as

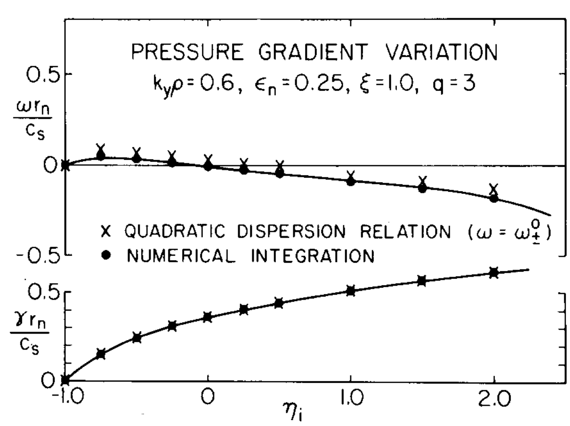

FIG. 4. Shows the variation of ω_k, γ_k with the ion pressure gradient, $1+\eta_i$, as obtained from the dispersion relation and numerical integration.

$(1+\eta)^{1/2}$ and is given approximately by Eq. (7) for k, ϵ_n, ξ, q in the range of the reference values. At small growth rates the hydrodynamic approximation for the ion behavior fails. The condition for validity of this approximation is obtained after a calculation of the mean parallel wavenumber in the normal mode wavefunction. Here, we note that the condition $\gamma > v_i/qR$ excludes the region $\gamma r_n/c_s \leq \epsilon_n/q = 0.083$ near the origin in Fig. 4.

Having established the accuracy of Eq. (7) we proceed to analyze the parametric dependence of the wavefunction. Through the parameter variations the modes were found to be localized to the outside of the torus. The characteristic angle $\bar{\theta}$ at which the mode amplitude is one-half its maximum value varies as $\bar{\theta} = \langle\theta^2\rangle^{1/2} = (\mathrm{Re}\,\sigma)^{-1/2}$ computed from Eqs. (2) and (7). In particular, we obtain for the characteristic mode width

$$\bar{\theta} = \frac{(2\epsilon_n)^{1/4}}{k\xi^{1/2}q^{1/2}(1+\eta)^{1/4}}\,. \tag{9}$$

For the reference case, Eq. (10) gives $\bar{\theta} = 0.68 = 40°$. Again the parameter dependence is verified for variations about the reference case.

The fact that $\bar{\theta}$ is inversely proportional to $k_\theta\rho = k$ is a significant feature of the modes. This feature could be useful in identifying the modes by microwave scattering measurements. This proportionality also implies that the average value of k_r for the modes is approximately independent of k_θ. From the wavefunction analysis in Sec. IVB of Ref. 1, we obtain that $\langle k_r\rangle = 0$ and that

$$\langle k_r^2\rangle^{1/2} = k_\theta\,\xi\,\bar{\theta}\,, \tag{10}$$

which for the localized modes gives

$$\bar{k}_r = \frac{(2\epsilon_n)^{1/4}\xi^{1/2}}{q^{1/2}(1+\eta)^{1/4}}\,. \tag{11}$$

For the reference case with $\bar{\theta} = 0.68$, $k = 0.6$, and $\xi = 1$, we have $\bar{k}_r = 0.41$. We note that $\bar{k}_r > k$ occurs for long wavelengths or strong shear according to Eq. (11).

Now we consider the average parallel wavenumber for the modes and the implied parallel phase velocity. The variation of the mode amplitude along the magnetic field is characterized by $\langle k_\parallel\rangle = 0$ and

$$\bar{k}_\parallel = \langle k_\parallel^2\rangle^{1/2} = \frac{\epsilon_n}{q\bar{\theta}} = \frac{\epsilon_n^{3/4}k\xi^{1/2}(1+\eta)^{1/4}}{q^{1/2}(1+k^2)^{1/2}}\,. \tag{12}$$

For the reference case we have $\bar{k}_\parallel r_n = \bar{k}_\parallel = 0.12$. The effective magnitude of the parallel phase velocity $|\omega/k_\parallel c_s| \sim \gamma/\bar{k}_\parallel c_s$ is given by

$$\frac{\gamma}{\bar{k}_\parallel c_s} = \frac{q^{1/2}(1+\eta)^{1/4}}{\xi^{1/2}\epsilon_n^{1/4}} > 1\,, \tag{13}$$

where the condition $\gamma > \bar{k}_\parallel c_s$ is required for the hydrodynamic approximation to apply. For the reference case the value is $\gamma/\bar{k}_\parallel c_s = 2.9$. The actual parallel phase velocity $\omega_k/\bar{k}_\parallel c_s$ is less than $\gamma/\bar{k}_\parallel c_s$. Due to the slow propagation speed of the wave compared with the Alfvén velocity and the electron thermal velocity, the electromagnetic and nonadiabatic electron effects are small perturbations in the wave. The most important correction of the parallel dynamics is the neglect of the ion temperature fluctuations driven by the finite parallel compression due to $\gamma_\parallel p_i \nabla_\parallel v_\parallel$ in the fluid equations.[11] The compressional effects substantially lower the growth rate of the lower phase velocity modes $|\omega| \gtrsim \bar{k}_\parallel v_i$.

IV. MODE COUPLING THEORY

Now, we consider the nonlinear hydrodynamic equations in a simple limit where only the convective nonlinearity in the ion pressure balance equation is retained. Other unpublished mode coupling studies and three-dimensional fluid simulations[11] for the pressure gradient driven mode in slab geometry, that apply to the high shear regime in Fig. 1, suggest that convective mixing of the pressure is the dominant nonlinear mechanism.

After transforming the equations into the standard dimensionless variables, we obtain the following mode coupling equations:

$$(1+k_\perp^2)\frac{d\varphi_{\mathbf{k}}}{dt} = -ik[1-k_\perp^2(1+\eta)]\,\varphi_{\mathbf{k}} - i\hat{k}_\parallel v_{\mathbf{k}} + 2ik\epsilon_n K(y)(\varphi_{\mathbf{k}} + p_{\mathbf{k}})\,, \tag{14}$$

$$\frac{dv_{\mathbf{k}}}{dt} = -i\hat{k}_\parallel(\varphi_{\mathbf{k}} + p_{\mathbf{k}})\,, \tag{15}$$

$$\frac{dp_{\mathbf{k}}}{dt} = -ik(1+\eta)\varphi_{\mathbf{k}} + \sum_{\mathbf{k}_1+\mathbf{k}_2=\mathbf{k}} (\mathbf{k}_1\times\mathbf{k}_2)_\parallel \varphi_{\mathbf{k}_1} p_{\mathbf{k}_2}\,, \tag{16}$$

where $k_\perp^2 = k^2 + k^2\xi^2y^2$, $\hat{k}_\parallel = -i(\epsilon_n/q)\partial/\partial y$, and $K(y) \simeq 1 + (\xi - 1/2)y^2$. In obtaining Eq. (14) we assume linear, adiabatic electrons and use quasi-neutrality to eliminate the fluctuating density in terms of the fluctuating potential.

The coupled nonlinear equations (14)–(16) are still rather complicated by the nonuniform toroidal geometry. Let us introduce a further approximation that eliminates these complications. We assume that the parallel flow $v_{\mathbf{k}}$ of the ions remains, as in linear theory, able to balance the shear, the poloidal variation and the radial wave propagation. Such a parallel motion would be governed by

$$\hat{k}_\parallel v_{\mathbf{k}} \cong 2k\epsilon_n(\xi - 1/2)y^2(\varphi_{\mathbf{k}} + p_{\mathbf{k}}) + k^3\xi^2(1+\eta)\,y^2\varphi_{\mathbf{k}} - k^2\xi^2y^2\dot{\varphi}_{\mathbf{k}}\,.$$

Under conditions where such a parallel flow occurs, the nonlinear problem reduces to the two dimensional mode coupling equations determined by

$$(1+k^2)\frac{d\varphi_{\mathbf{k}}}{dt} = -iku_{\mathbf{k}}\varphi_{\mathbf{k}} + 2ik\epsilon_n p_{\mathbf{k}}\,, \tag{17}$$

$$\frac{dp_{\mathbf{k}}}{dt} = -ik(1+\eta)\varphi_{\mathbf{k}} + \sum_{\mathbf{k}_1+\mathbf{k}_2=\mathbf{k}} (\mathbf{k}_1\times\mathbf{k}_2)_\parallel \varphi_{\mathbf{k}_1} p_{\mathbf{k}_2}\,, \tag{18}$$

where we defined

$$u_{\mathbf{k}} = 1 - k^2(1+\eta) - 2\epsilon_n \quad \text{and} \quad \gamma_0^2 = 2\epsilon_n(1+\eta)\,.$$

We define the spectral distribution of the two point potential correlation functions as $I(k_x, k_y, \omega)$. Using the linearity of Eq. (17), it is straightforward to reduce the coupled system (17) and (18) to the standard form

$$\epsilon_k(\omega)\varphi_k + \sum_{k_1+k_2=k} \epsilon^{(2)}_{k_1,k_2}\varphi_{k_1}\varphi_{k_2} = 0\,, \tag{19}$$

where $k=(k_x, k_y, \omega)$ and

$$\epsilon_k(\omega) = \omega^2(1+k^2) - \omega k u_k + k^2\gamma_0^2\,,$$

$$\epsilon^{(2)}_{k_1,k_2} = \frac{ik}{2}(\mathbf{k}_1\times\mathbf{k}_2)_\parallel\left(u_{k_2} - u_{k_1} - \frac{\omega_2}{k_2} + \frac{\omega_1}{k_1}\right).$$

We assume that the nonlinear interaction produces weak correlations among the normal modes $\epsilon_k(\omega)=0$, and we ask for the nonlinear dispersion relation that takes into account the broad spectrum of linearly unstable modes given in Sec. III.

From a truncation of the four field correlation function in terms of the pair correlation function $I(\mathbf{k},\omega)=I_k$ we obtain the well-known renormalized dispersion relation

$$\epsilon_k^{\mathrm{nl}} = \epsilon_k - \sum_{\mathbf{k}_1}\int_{-\infty}^{+\infty}\frac{d\omega_1}{2\pi}\,\frac{4\epsilon^{(2)}(k_1, k-k_1)\epsilon^{(2)}(-k_1,k)I_{k_1}}{\epsilon^{\mathrm{nl}}_{k-k_1}}\,. \tag{20}$$

For the present calculation we shall assume that due to the broad unstable spectrum it is adequate to approximate the response function $1/\epsilon^{\mathrm{nl}}_{k-k_1}$ by $1/\epsilon_{k-k_1}$ under the interaction integral. In the terminology of Horton and Choi[12] this is the simply renormalized theory.

In this section we are concerned with deriving from $\epsilon_k^{\mathrm{nl}}=0$ the conditions imposed on the fluctuation spectrum to have marginally stable roots. We assume, and verify *a posteriori*, that the fluctuation spectrum is peaked in azimuthal wavenumber at $k=\bar{k}<k_0<1$ where k_0 is defined by $u_{k_0}=0$ and is the center of the region of linear growth. In the calculation of the interaction integral it is sufficient to approximate the frequencies by the linear values $\omega(k)$ which are analyzed in Secs. II and III. In the region of growth the frequency is given approximately by $\omega(k)=i|k|\gamma_0$ in the region $|k|\le k_0$. Similarly, the response function ϵ_{k-k_1} is given approximately by $\epsilon_{k-k_1}\cong(\omega_k-\omega_{k_1})^2+(k-k_1)^2\gamma_0^2$. Correction terms are higher order in $|u_{\bar{k}}/\gamma_0|$ and $I_{\bar{k}}$. With these simplifications we obtain

$$\epsilon^{(2)}_{k_1,k-k_1} = -\gamma_0 k(\mathbf{k}_1\times\mathbf{k})_\parallel \times \begin{Bmatrix} 1, & \text{for } 0<k<k_1 \\ -1, & \text{for } k<k_1<0 \\ 0, & \text{otherwise} \end{Bmatrix},$$

$$\epsilon^{(2)}_{-k_1,k} = \gamma_0(k-k_1)(\mathbf{k}_1\times\mathbf{k})_\parallel \times \begin{Bmatrix} 1, & \text{for } k \text{ and } k_1>0 \\ -1, & \text{for } k \text{ and } k_1<0 \\ 0, & \text{otherwise} \end{Bmatrix}, \tag{21}$$

and $\epsilon_{k-k_1}=-4\gamma_0^2 kk_1$ for $kk_1>0$. With these results the nonlinear dispersion relation (20) reduces to

$$\epsilon_k^{\mathrm{nl}}(\omega) = \omega(\omega-ku_k)+k^2\gamma_0^2 + \int_{-\infty}^{+\infty}dk_x\int_k^\infty dk_1\,\frac{(\mathbf{k}\times\mathbf{k}_1)_\parallel^2\,k(k-k_1)I(\mathbf{k}_1)}{kk_1}\,, \tag{22}$$

for $k>0$.

We model the radial wavenumber spectrum to reduce the mode coupling to a one dimensional problem. From the linear properties of the wavefunctions given in Sec. III we observe that there is a well defined radial wavenumber $\langle k_x^2\rangle^{1/2}=\bar{k}_r$ given in Eq. (11) for the entire spectrum of azimuthal wavenumbers k. Thus, we are led to investigate azimuthal mode coupling in a spectrum characterized by its lowest moments in k_x. Taking the spectrum as symmetric in k_x with $I(k_x,k_y)=I(k_x^2,k)$ and peaked about $\langle k_x^2\rangle$, we write that

$$I(k)=\int_{-\infty}^{+\infty}dk_x\,I(k_x^2,k)=2\int_0^\infty dk_x\,I(k_x^2,k)\,,$$

and

$$\langle k_x^2\rangle I(k)=2\int_0^\infty dk_x\,k_x^2\,I(k_x^2,k)\,,$$

with the subsequent approximation made that $\langle k_x^2\rangle$ is determined by the toroidal mode structure.

In the turbulent state the linearly unstable part of the spectrum is balanced by the interaction integral when the one-dimensional spectrum $I(k)$ satisfies the equation

$$\omega(\omega-ku_k)+k^2\gamma_0^2-\langle k_x^2\rangle\int_k^\infty\frac{dk_1}{k_1}(k_1-k)(k^2+k_1^2)I(k_1)=0\,. \tag{23}$$

The shorter scale length turbulence $I(k_1)$ at $k_1>k$ reacts on the fluctuation at a given k as shown by a less formal calculation in the Appendix. As the magnitude of $I(k_1)$ increases the growth rate from Eq. (23) decreases until marginal stability is reached with $\omega=\frac{1}{2}ku_k$ and

$$k^2(\gamma_0^2-\tfrac{1}{4}u_k^2)=\langle k_x^2\rangle\int_k^\infty\frac{dk_1}{k_1}(k_1-k)(k^2+k_1^2)I(k_1) \tag{24}$$

that follows from Eq. (23) in the unstable domain $|u_k|<2\gamma_0$. From another point of view we may solve the quadratic equation (23) for $\omega=\omega(k,I)$ and find that when the spectrum satisfies Eq. (24) the oscillations have neutral stability with $\omega\simeq\frac{1}{2}ku_k$.

The principal features of the spectrum $I(k)$ satisfying Eq. (24) are readily determined. The broadest spectrum that leaves the interaction integral well defined, to within logarithmic terms, varies as $I(k)=I_0/k$ for $k\ll1$ and as I_1/k^3 for large k. Examining the equation for power law distributions shows that the distribution I_0/k down to a cutoff wavenumber k_c allows the interaction term to balance the driving term. We now simplify Eq. (24) by dropping the term $u_k^2/4$ compared with γ_0^2 which is a good approximation in the strongest growing part of the unstable spectrum. An integral constraint follows by acting on Eq. (24) with $\int_0^\infty dk\,I(k)$. Recognizing that $\bar{k}\ll1$ the constraint can be solved approximately for the result that

$$\langle\varphi^2\rangle=\int_0^\infty I(k)dk=\frac{\gamma_0^2}{2\langle k_x^2\rangle}\,. \tag{25}$$

From Eq. (25) it follows that the constant I_0 is

$$I_0=\gamma_0^2/2\langle k_x^2\rangle\Lambda \tag{26}$$

where $\Lambda=\ln(k_0/k_c)$ and the continuity of $I(k)$ implies the constant $I_1=k_0^2I_0$. The result Eq. (26) also follows from substituting $I(k)=I_0/k$ for $k_c\le k\le k_0$ into Eq. (25). The limit on the width of the spectrum for the existence of $\langle\mathbf{E}^2\rangle$ is the same, in this model as the existence of the interaction integral in Eq. (24) since

$$\langle E_y^2\rangle = \int dk_x\, dk_y\, k_y^2 I(k_x, k_y) = 2\int_0^\infty dk\, k^2 I(k)$$
$$\sim 2I_1 \ln(k_{\max}),$$

for the I_1/k^3 spectrum.

From these features we arrive at the conclusion that the azimuthal wavenumber spectrum is as shown in Fig. 5. The precise value of the cutoff wavenumber k_c remains to be determined. Here, we assume that it occurs where $|\omega_{\mathbf{k}}| \sim v_i/qR$ at which point the kinetic phenomena in the ion dynamics becomes important. This limitation to the hydrodynamic regime is discussed in Sec. III.

Finally, it is important to observe that the original mode coupling equations (17) and (18) have an exact constant of the motion

$$\langle \varphi^2\rangle - \frac{2\epsilon_n}{1+\eta}\langle \delta p^2\rangle = \text{const}. \tag{27}$$

Neglecting the initial fluctuation level, the integral of the motion relates the amplitude of the potential and pressure fluctuations. From the root-mean-square potential fluctuation $\varphi_0 = \langle\varphi^2\rangle^{1/2} = \gamma_0/\sqrt{2}\,\langle k_x^2\rangle^{1/2}$ given by Eq. (25), we obtain that the amplitude of the pressure fluctuation $\delta p_0 = \langle \delta p^2\rangle^{1/2}$ is given by

$$\bar{k}_x\, \delta p_0 = \frac{1}{\sqrt{2}}\left|\frac{dp}{dx}\right| \tag{28}$$

to within a logarithmic factor. The relationship in (28) is the well-known mixing-length result commonly invoked to estimate the amplitude of drift-wave turbulence. The result is derived here from the reduced mode coupling equations and the assumption of a well defined average wavenumber in the k_x spectrum.

In regard to the present modeling of the two-dimensional spectrum, we note that even in the simpler problem of ion acoustic turbulence no two dimensional analytic solutions are known.[12] As to justification of the present model, we note that the assumptions of the dominant nonlinear process and the k_x spectrum peaked about the linear $\langle k_x^2\rangle^{1/2}$ are motivated by the three-dimensional sheared slab simulations of Ref. 11. Basically, the model reflects the observations from the initial value problem starting with small amplitude linear eigenfunctions that the azimuthal wavenumber spectrum deforms more rapidly than the radial wavenumber spectrum during saturation of the growth of the pressure fluctuations. Here, we determine the deformation of the azimuthal wavenumber spectrum required for nonlinear stability. The one-dimensional equation (24), based on a weak turbulence approximation in evaluating $1/\epsilon^{\mathrm{nl}}_{\mathbf{k}-\mathbf{k}_1}$ with $1/\epsilon_{\mathbf{k}-\mathbf{k}_1}$ under the k_1 integral in Eq. (20), does not adequately describe some features of the turbulent spectrum as pointed out by the referees and discussed in more detail in Appendix B.

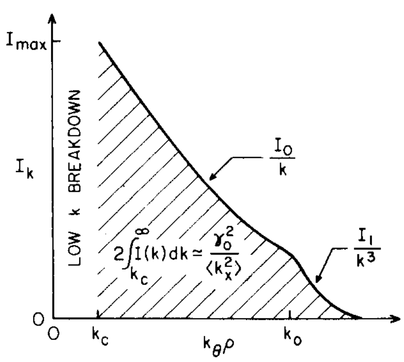

FIG. 5. The approximate form of the azimuthal mode number spectrum that takes the renormalized dispersion relation $\epsilon^{\mathrm{nl}}_{\mathbf{k}}(\omega, I) = 0$ to marginal stability. The constants I_0, I_1 and k_c, k_0 are discussed in Sec. IV.

V. QUASI-LINEAR TRANSPORT

The normal mode equation (1), is consistent with the following linearized hydrodynamic equations for the normalized ion density $n_{i\mathbf{k}}$ fluctuation, the parallel ion velocity $v_{\mathbf{k}}$ fluctuation, and the ion pressure $p_{\mathbf{k}}$ fluctuation:

$$n_{ik} = \frac{k}{\omega}\varphi_{\mathbf{k}} - k_\perp^2(y, y_0)(\varphi_{\mathbf{k}} + p_{\mathbf{k}}) - \frac{2k\epsilon_n}{\omega} K(y, y_0)(\varphi_{\mathbf{k}} + p_{\mathbf{k}}) + \frac{\hat{k}_\parallel v_{\mathbf{k}}}{\omega}, \tag{29}$$

$$v_{\mathbf{k}} = \hat{k}_\parallel(\varphi_{\mathbf{k}} + p_{\mathbf{k}})/\omega, \tag{30}$$

$$p_{\mathbf{k}} = [k(1+\eta)/\omega]\varphi_{\mathbf{k}}, \tag{31}$$

where $k_\perp^2(y, y_0) = k^2 + k^2\xi^2(y-y_0)^2$, $K(y, y_0) = \cos y + \xi(y-y_0)\sin y$, and $\hat{k}_\parallel = -i(\epsilon_n/q)\partial/\partial y$.

For nondissipative, adiabatic electron response, $n_{e\mathbf{k}} = \varphi_{\mathbf{k}}$, the condition of quasi-neutrality $n_{e\mathbf{k}} = n_{i\mathbf{k}}$ yields the normal mode equation (1). From the space-time average of the hydrodynamic equations we find the anomalous particle flux

$$\Gamma = \langle n v_{Ex}\rangle = \frac{\rho}{r_n}\frac{cT}{eB}\sum_{\mathbf{k}} ik\varphi_{\mathbf{k}}^* n_{\mathbf{k}} = 0, \tag{32}$$

since $\varphi_{\mathbf{k}}$ and $n_{\mathbf{k}}$ are in phase in the absence of electron dissipation.

The anomalous ion thermal flux is

$$q = \langle p v_{Ex}\rangle = \frac{\rho}{r_n}\frac{cT}{eB}\sum_{\mathbf{k}} ik\varphi_{\mathbf{k}}^* p_{\mathbf{k}} = -\frac{\rho}{r_n}\frac{cT}{eB}\int d\mathbf{k}\,\frac{k^2\gamma_{\mathbf{k}} I(\mathbf{k})}{\omega_{\mathbf{k}}^2 + \gamma_{\mathbf{k}}^2}\frac{dp}{dx} = -\frac{\rho}{r_n}\frac{cT}{eB}\hat{\chi}_i\frac{dp}{dx}, \tag{33}$$

where $\hat{\chi}_i$ is a function of ϵ_n, ξ, η, and q. In obtaining Eq. (33) the linear approximation for the pressure-potential phase relationship, namely (31), is used under the spectral integral. Since the peak of the spectrum occurs where this linear frequency $\omega(k)$ relation is given by $\gamma_{\mathbf{k}} \simeq |k|\gamma_0 > \omega_{\mathbf{k}}$, the dimensionless thermal conductivity reduces to

$$\hat{\chi}_i = \frac{1}{\gamma_0}\int_0^\infty kI(k)dk, \tag{34}$$

where $I(k)$ is the one-dimensional azimuthal spectrum analyzed in Sec. IV.

From formula (34) we see that all components of the $1/k$ part of the wavenumber spectrum shown in Fig. 5

contribute equally to the thermal conductivity $\hat{\chi}_i$. The contribution to $\hat{\chi}_i$ from the I_0/k component of the spectrum is $I_0(k_0-k_c)$ and that from the I_1/k^3 component is I_1/k_0 which equals $I_0 k_0$. For $k_c \ll k_0$, the total contribution to the integral is thus

$$\hat{\chi}_i = 2I_0 k_0/\gamma_0$$

which, upon substituting for I_0 from Eq. (26), yields

$$\hat{\chi}_i = k_0\gamma_0/\langle k_x^2\rangle\Lambda\,, \qquad (35)$$

where $k_0\gamma_0$ is essentially the maximum linear growth rate γ_{k_0}. Thus, we find that the spectral distribution obtained in Sec. IV together with the quasi-linear formula for the thermal flux reproduces, to within a logarithmic factor Λ for this problem, the familiar Kadomtsev estimate for the anomalous diffusion.

Now, we compare the anomalous ion thermal conductivity given by Eqs. (33) and (35) with the neoclassical plateau formula

$$\chi_i^{nc} = 2.6(\rho_i q)^2\,\frac{v_i}{qR} = 2.6\,\frac{\rho}{r_n}\,\frac{cT}{eB}\,q\epsilon_n\,.$$

Using Eq. (11) for $\langle k_x^2\rangle = \bar{k}_r^2$, we obtain from Eq. (33) the result that

$$\chi_i = \frac{\rho}{r_n}\,\frac{cT}{eB}\,\frac{q(1+\eta)^{1/2}}{\xi} \qquad (36)$$

to within a numerical factor of order unity. The anomalous transport exceeds the neoclassical plateau transport by the factor $(1+\eta)^{1/2}/\xi\epsilon_n$ which is typically a factor of order five to ten.

Evidently, the toroidal curvature ion pressure gradient driven drift mode is capable of producing an anomalous ion thermal conductivity which scales with density, temperature and safety factor as the plateau neoclassical formula. The rate of the anomalous transport is at least several times faster than the collisional rate. We recall that there is experimental evidence for an anomalous ion thermal conductivity in the ion power balance studies for the neutral beam heated plasmas in the TFR[13] and, possibly, the PLT[14] experiments. The TFR Group reports that χ_i is an increasing function of ion temperature within their experimental range, in contrast with the neoclassical conductivity χ_i^{nc} which decreases with temperature. In the power balance scheme that gives the most consistent interpretation of the radial plasma profiles, the TFR Group reports in Figs. 36–38 of Ref. 13 that both the hydrogen and deuterium plasma show an anomaly factor range from 5 to 15 and centered around 10. Such an enhancement in χ_i would appear consistent with the drift-wave turbulent ion conductivity derived in this work.

For a multiple ion species plasma it is the *total ion pressure gradient* that drives the instability. The cross-field scale length ρ of the fluctuations is determined by the ion mass density or $\langle m_i\rangle = \Sigma_i n_i m_i/n_e$ where the electron density is $n_e = \Sigma_i n_i Z_i$.

VI. CONCLUSIONS

In the presence of vigorous auxiliary ion heating, such as in neutral beam injection[13,14] or for the quasi-steady fusion burn profiles, e.g., Fig. 3 of Ref. 15, found in reactor studies, it is typical to have the ion temperature gradient greater than the density gradient. Such peaked ion temperature profiles are unstable to ballooning drift waves. In Sec. II we analyze the toroidal normal mode equation for these ion pressure gradient driven drift waves. We show that in the hydrodynamic regime $|\omega| > v_i/qR$ the characteristics of the instability, such as its poloidal localization and mean parallel and radial wavenumbers, are given by simple formulae. By numerical integrations in Sec. III, the parametric variation of the growth rate with shear, aspect ratio, and the ion temperature-to-density gradient ratio is shown to agree with the growth rate formula.

The localization of drift waves by ion curvature drifts has been pointed out in earlier work on shearless multipoles.[9] It should also be mentioned that the linear characteristics of the ion pressure gradient driven modes are analyzed at low shear with quadratic forms in the radially local approximation in Ref. 8 and in a recent nonlocal analysis in Ref. 16. The primary emphasis in Secs. II and III of the present work is (i) on developing an appropriate toroidal normal mode analysis of this instability which can be extended to a nonlinear mode-coupling theory and (ii) to establish the essential parametric dependences of such eigenmodes and the associated fluctuations.

Drawing from the fact that the basic mode characteristics given in Sec. II and III are explained by fluid equations containing the local unfavorable ion drift and drawing from the three-dimensional fluid simulations[11] for the analogous slab problem, we develop a simple set of two-dimensional mode coupling equations in Sec. IV for the nonlinear regime. In Sec. IV we apply simply renormalized turbulence theory to the reduced problem to obtain a nonlinear dispersion relation. After introducing a model for the radial wavenumber spectrum, it is shown that for the azimuthal wavenumber spectrum given in Fig. 5 the renormalized dispersion relation $\epsilon_k^{nl}(\omega, I) = 0$ describes marginally stable oscillations.

For the spectral distribution obtained in Sec. IV we evaluate the quasi-linear formulae for the anomalous ion thermal conductivity χ_i in Sec. V. In the evaluation of the thermal conductivity χ_i it is assumed adeqaute to use the linear phase relationship between the pressure and the potential fluctuations. As shown by simulation studies,[11] a well-defined steady state of transport is produced by the drift-wave instability. Within this framework, a final formula is obtained for the anomalous ion thermal conductivity. The anomalous conductivity scales with density, temperature and safety factor as the neoclassical plateau formula. The anomalous transport rate exceeds the neoclassical rate by a factor of the order of the aspect ratio.

ACKNOWLEDGMENTS

The authors wish to express their thanks to Paul Terry and Bill Anderson for help with the analysis.

The work was supported by the U.S. Department of Energy.

APPENDIX A

The nonlinear dispersion relation $\epsilon_k^{nl}(\omega)$ given in Eq. (23) of Sec. IV shows that the reaction of the fluctuation spectrum is on the long azimuthal wavelength components of the spectrum. This effect, which is given by Eq. (21) in turbulence theory, can be seen less formally by calculating the nonlinear interaction term for two modes $\mathbf{k}_1$ and $\mathbf{k}_2$. In the region of low azimuthal phase velocities, we may write the eigenfunctions as

$$\begin{bmatrix} \varphi(\mathbf{r},t) \\ p(\mathbf{r},t) \end{bmatrix} = \varphi(t) \begin{bmatrix} \sin(qx)\cos(ky) \\ \mathrm{sg}(k)[(1+\eta)/2\epsilon_n]^{1/2}\sin(qx)\sin(ky) \end{bmatrix}, \quad \text{(A1)}$$

where $\mathrm{sg}(x)=\pm 1$ for $x \gtrless 0$, respectively. Consider the interaction $\mathbf{k}_1+\mathbf{k}_2=\mathbf{k}$ by calculating $\hat{z}\cdot\nabla_\perp\varphi\times\nabla_\perp\delta p = [\varphi_1+\varphi_2, \delta p_1+\delta p_2] = [\varphi_1, \delta p_2]+[\varphi_2, \delta p_1]$. After a straightforward calculation we obtain

$$\varphi_1(t)\varphi_2(t)[(1+\eta)/2\epsilon_n]^{1/2}(q_1k_2+q_2k_1) \times \sin(qx)\cos[(|k_1|-|k_2|)y]. \quad \text{(A2)}$$

Due to the phase relationship between φ and δp only the difference wavenumber $|k_1|-|k_2|$ is generated. Applying this result to the interaction of $k>0$ and $k_1>0$ we obtain the first interaction at $\cos[(k-k_1)y]$ and the second interaction at $k=|k_1|-|k-k_1|$ only when $k_1>k$.

APPENDIX B

In this appendix it is shown that the reduced mode coupling equation can be solved to obtain a model azimuthal wavenumber spectrum. The model spectrum is singular at the modes of marginal stability.

In the reduced one-dimensional equation (24) the azimuthal spectrum is determined by

$$\int_k^\infty \frac{dk_1}{k_1}(k_1-k)(k^2+k_1^2)I(k_1) = \begin{cases} \dfrac{\gamma_k^2}{\langle k_x^2\rangle}, & \text{for } \gamma_k^2 \geq 0, \\ 0, & \text{for } \gamma_k^2 < 0, \end{cases} \quad \text{(B1)}$$

where the fluid theory growth rate is given by $\gamma_k^2 = k^2(\gamma_0^2 - \frac{1}{4}u_k^2)$ with $u_k = 1-2\epsilon_n - k^2(1+\eta)$. The growth rate is factored according to

$$\gamma_k^2 = k^2(k^2+k_1^2)(k_2^2-k^2)\tfrac{1}{4}(1+\eta)^2, \quad \text{for } 0 \leq k^2 \leq k_2^2,$$

with

$$k_1^2 = \frac{2\gamma_0-(1-2\epsilon_n)}{1+\eta},$$

$$k_2^2 = \frac{2\gamma_0+(1-2\epsilon_n)}{1+\eta},$$

with both k_1^2 and k_2^2 positive for typical parameters. Due to the positive definite kernel Eq. (B1) implies that $I(k)=0$ for $k>k_2$.

We now scale the wavenumber distribution to the marginal mode k_2 and the amplitude of the distribution by writing

$$\xi = \frac{k}{k_2} \quad \text{and} \quad \alpha = \frac{k_1^2}{k_2^2} = \frac{2\gamma_0-1+2\epsilon_n}{2\gamma_0+1-2\epsilon_n}$$
$$I(k) = [(1+\eta)^2/4\langle k_x^2\rangle]k_2^3\hat{I}(\xi,\alpha). \quad \text{(B2)}$$

With these scalings (B2) the spectral equation (B1) becomes

$$\int_\xi^1 \frac{d\xi_1}{\xi_1}(\xi_1-\xi)(\xi^2+\xi_1^2)\hat{I}(\xi_1) = \xi^2(\xi^2+\alpha)(1-\xi^2), \quad \text{(B3)}$$

for $\xi<1$. Considering the derivatives of Eq. (B3) evaluated at $\xi = 1-0^+$, it becomes evident that $\hat{I}(\xi)$ must contain a singularity at $\xi=1$. Thus, we write

$$\hat{I}(\xi) = A\delta(\xi-1)+\tilde{I}(\xi), \quad \text{(B4)}$$

and obtain an equation for $\tilde{I}(\xi)$ by computing the first four derivatives of Eq. (B3). Substituting (B4) into (B3) and computing the derivatives yields

$$\int_\xi^1 \frac{d\xi_1}{\xi_1}(2\xi\xi_1-3\xi^2-\xi_1^2)\tilde{I}(\xi_1)+A(2\xi-3\xi^2-1) = 2\alpha\xi+4(1-\alpha)\xi^3-6\xi^5, \quad \text{(B5)}$$

$$\int_\xi^1 \frac{d\xi_1}{\xi_1}(2\xi_1-6\xi)\tilde{I}(\xi_1)+2\xi\tilde{I}(\xi)+(2-6\xi)A = 2\alpha+12(1-\alpha)\xi^2-30\xi^4, \quad \text{(B6)}$$

$$-6\int_\xi^1 \frac{d\xi_1}{\xi_1}\tilde{I}(\xi_1)+4\tilde{I}(\xi)+2\frac{d}{d\xi}[\xi\tilde{I}(\xi)]-6A = 24(1-\alpha)\xi-120\xi^3, \quad \text{(B7)}$$

$$\frac{6}{\xi}\tilde{I}(\xi)+4\frac{d\tilde{I}}{d\xi}+2\frac{d^2}{d\xi^2}[\xi\tilde{I}] = 24(1-\alpha)-360\xi^2. \quad \text{(B8)}$$

The solutions of the homogeneous part of Eq. (B8) are ξ^λ with $\lambda = (-3 \pm i\sqrt{3})/2$, and the general solution of (B8) is

$$\tilde{I}(\xi) = B\xi^{-3/2}\cos[(\sqrt{3}/2)\ln\xi - C] + \tfrac{12}{7}(1-\alpha)\xi - \tfrac{60}{7}\xi^3. \quad \text{(B9)}$$

The constants A, B, and C are determined by evaluating Eqs. (B5), (B6), and (B7) with (B9) at $\xi=1$. Carrying out the algebra gives

$$A = 1+\alpha, \quad B = \tfrac{2}{7}(1+6\alpha+21\alpha^2)^{1/2},$$
$$\tan C = \sqrt{3}(1+\alpha)/(1+9\alpha). \quad \text{(B10)}$$

The dominant features of the model spectrum are singularities at the marginal modes $k=0$ and $k=k_2$ and the $k^{-3/2}$ variation in the linearly unstable domain between $k=0$ and k_2. The unphysical features of this model spectrum, namely the singularities and the negative values of the spectrum at small $\xi=k/k_2$, suggest the need to reconsider the use of the weak turbulence approximation and the ansatz used to decouple the radial and azimuthal spectral distributions in future work.

[1] D. I. Choi and W. Horton, Phys. Fluids 23, 356 (1980).
[2] R. J. Hastie, K. W. Hesketh, and J. B. Taylor, Nucl. Fusion 19, 1223 (1979).
[3] E. A. Frieman, G. Rewoldt, W. M. Tang, and A. H. Glasser, Phys. Fluids 23, 1750 (1980).
[4] L. Chen and C. Z. Cheng, Phys. Fluids 23, 2242 (1980).
[5] W. Horton, R. Estes, H. Kwak, and D. I. Choi, Phys. Fluids 21, 1366 (1978).
[6] G. Rewoldt, W. M. Tang, and E. A. Frieman, Phys. Fluids 21, 1513 (1978).
[7] B. Coppi, M. N. Rosenbluth, and R. Z. Sagdeev, Phys. Fluids

10, 582 (1967).
[8]B. Coppi and F. Pegoraro, Nucl. Fusion **17**, 5 (1977).
[9]P. H. Rutherford and E. A. Frieman, Phys. Fluids **11**, 569 (1968).
[10]J. W. Connor, R. J. Hastie, and J. B. Taylor, Proc. R. Soc. London Ser. A **365**, 1 (1979).
[11]W. Horton, R. D. Estes, and D. Biskamp, Plasma Phys. **22**, 663 (1980).
[12]W. Horton and D. I. Choi, Phys. Report **49**, 273 (1979).
[13]Equipe TFR, Nucl. Fusion **18**, 1271 (1978).
[14]H. Eubank, R. Goldston, V. Arunasalam, M. Bitter, K. Bol, D. Boyd *et al.* in *Plasma Physics and Controlled Nuclear Fusion Research* (International Atomic Energy Agency, Vienna, 1979), Vol. I, p. 167.
[15]R. G. Mills, in *Technology of Controlled Thermonuclear Fusion Experiments*, edited by E. L. Draper (Technical Information Center, United States Department of Energy, Washington, D. C., 1974), p. 1.
[16]P. N. Guzdar, L. Chen, W. M. Tang, and P. H. Rutherford, Princeton Plasma Physics Report PPPL-1601 (1980).